3894–3907 Nucleic Acids Research, 2014, Vol. 42, No. 6 Published online 9 January 2014
doi:10.1093/nar/gkt1361

Binary recombinase systems for high-resolution conditional mutagenesis

Mario Hermann[1,2], Patrick Stillhard[1], Hendrik Wildner[3], Davide Seruggia[4,5], Viktor Kapp[1], Héctor Sánchez-Iranzo[6], Nadia Mercader[6], Lluís Montoliu[4,5], Hanns Ulrich Zeilhofer[3,7] and Pawel Pelczar[1,*]

[1]Institute of Laboratory Animal Science, University of Zurich, Sternwartstrasse 6, CH-8091 Zurich, Switzerland, [2]Institute of Neuropathology, University Hospital of Zurich, Schmelzbergstrasse 12, CH-8091 Zurich, Switzerland, [3]Institute of Pharmacology and Toxicology, University of Zurich, Winterthurerstrasse 190, CH-8057 Zurich, Switzerland, [4]National Centre for Biotechnology (CNB-CSIC), Darwin 3, 28049 Madrid, Spain, [5]CIBERER-ISCIII, Darwin 3, 28049 Madrid, Spain, [6]Program of Cardiovascular Development, Department of Cardiovascular Development and Repair, Centro Nacional de Investigaciones Cardiovasculares Carlos III, calle Melchor Fernández Almagro 3, 28029 Madrid, Spain and [7]Institute of Pharmaceutical Sciences, Swiss Federal Institute of Technology (ETH) Zurich, Winterthurerstrasse 190, CH-8057 Zurich, Switzerland

Received July 8, 2013; Revised December 5, 2013; Accepted December 6, 2013

ABSTRACT

Conditional mutagenesis using Cre recombinase expressed from tissue specific promoters facilitates analyses of gene function and cell lineage tracing. Here, we describe two novel dual-promoter-driven conditional mutagenesis systems designed for greater accuracy and optimal efficiency of recombination. Co-Driver employs a recombinase cascade of Dre and Dre-respondent Cre, which processes loxP-flanked alleles only when both recombinases are expressed in a predetermined temporal sequence. This unique property makes Co-Driver ideal for sequential lineage tracing studies aimed at unraveling the relationships between cellular precursors and mature cell types. Co-InCre was designed for highly efficient intersectional conditional transgenesis. It relies on highly active trans-splicing inteins and promoters with simultaneous transcriptional activity to reconstitute Cre recombinase from two inactive precursor fragments. By generating native Cre, Co-InCre attains recombination rates that exceed all other binary SSR systems evaluated in this study. Both Co-Driver and Co-InCre significantly extend the utility of existing Cre-responsive alleles.

INTRODUCTION

Conditional mutagenesis in mice typically employs the Cre recombinase, which is expressed in a spatially and temporally restricted manner (1). Distinct Cre expression profiles result from the transcriptional control exercised by regulatory elements of well characterized promoters that are used to drive expression of conventional transgenes or of large fragments of genomic DNA that are routinely used to generate BAC transgenics (2). Alternatively, the fidelity of expression can be assured by directly inserting the Cre protein-coding sequence into a native gene locus using gene-targeting. Cre driver mouse lines generated with any of these strategies can be crossed to a wide variety of mice carrying Cre-responsive alleles. Depending on the responder allele, the Cre driver can mediate either gene ablation through the removal of *loxP*-flanked (floxed) coding sequences or gene activation caused by the removal of floxed STOP cassettes (1). Although elegant, conditional mutagenesis approaches are sometimes limited, as the regulatory elements of a single gene not always suffice for directing Cre to distinct subsets of cells in complex organs such as the brain or the immune system.

One way of enhancing the specificity of conditional somatic mutagenesis has been the development of the CreERT2 system, which allows temporal regulation of recombination through timed administration of tamoxifen (3). While this approach has allowed labeling and tracking of cells with increased temporal precision, it is still limited to cell populations that can be targeted by a single-promoter strategy. To date two strategies have been developed to enable dual-promoter transcriptional control of site-specific recombinases (SSRs), which can be broadly summarized as binary SSRs. The Cre reconstitution approach is based on splitting Cre into inactive polypeptide chains, expressing

*To whom correspondence should be addressed. Tel: +41 44 255 3737; Fax: +41 44 255 4421; Email: pawel.pelczar@ltk.uzh.ch

these fragments from two individual tissue-specific promoters and allowing the assembly of active Cre in cells where the transcriptional profiles of both promoters intersect. Several Cre reconstitution strategies have been described. Namely, the spontaneous reassembly of Cre fragments by α-complementation (4), fusing Cre fragments to protein dimerization domains to enhance Cre reassembly (5–8) or covalent reconstitution of Cre with the help of split-intein-mediated protein trans-splicing (9). All Cre reconstitution strategies strictly depend on promoters that allow simultaneous expression of the inactive Cre fragments. However, another intersectional dual-promoter strategy that combines two orthogonally active SSRs, Cre and Flp, allows promoters with non-overlapping temporal profiles to be used for restricting reporter expression. The Cre/Flp strategy employs reporter constructs that carry *loxP*- and *frt*-flanked STOP cassettes in various configurations (10) to selectively label cell sub-populations. Although elegant, this approach is generally not applicable to generate conditional knockout mice since conditional alleles usually only contain *loxP* sites that facilitate removal of exon sequences (1). In addition, *frt* sites are now frequently found in conditional alleles as a result of their assembly by recombineering (11,12), thus severely limiting the application of Flp-mediated conditional transgenesis in the mouse and restricting its use to lineage tracing studies using Cre/Flp-responsive reporter alleles. The phage D6 recombinase Dre (13) faithfully processes its cognate recognition sites known as *rox* sites and does not cross-react with *loxP* sites in transgenic mice (14). Thus, Dre represents a potential alternative to Flp for achieving dual-recombinase conditional transgenesis, however, Cre/Dre-responsive reporter genes have not been reported so far.

In this study, we describe the development of two novel binary SSR systems with the focus on achieving optimal binary recombination efficiency. The Co-Driver system is based on the SSRs Dre and Cre linked in a cascade that can be expressed from two independent promoters. Briefly, the Dre recombinase acts as a 'co-driver' and activates the Dre-regulated Cre driver gene, Roxed-Cre, which in turn leads to Cre-mediated output. The Co-Driver system not only restricts Cre-specific recombination to a subset of cells defined by the two promoters driving SSR expression but more importantly will only generate output if these promoters are co-expressed or expressed in a predetermined temporal sequence where Co-Driver SSR activity precedes that of the driver. This unique property makes Co-Driver ideal for sequential lineage tracing studies aimed at unraveling the relationships between cellular precursors and mature cell types.

We also developed a second, complementary approach, termed Co-InCre, which achieves highly effective Cre reconstitution promoted by gp41-1 split-inteins (15,16). The efficiencies of Co-Driver and Co-InCre in recombining a genomic *loxP*-flanked reporter were compared to Cre as well as previously reported Split-Cre systems (6,9). By using standardized expression constructs and transfections of a reporter cell line for all binary SSRs in combination with flow cytometry-based analysis of single cells we could show that Co-Driver functions on par with current Split-Cre systems, while Co-InCre significantly improved binary recombination efficiency by up to 2.5-fold. Constitutively expressed Co-Driver and Co-InCre triggered extensive recombination when introduced into the developing brains of Ai14 reporter mice (11). Co-Driver also facilitated the sequential linkage of two expression constructs based on the human glia-fibrillary acidic protein (hGFAP)-promoter (17) and the Thy1.2 expression cassette (18), respectively, which are differentially regulated during neocortical development. The Cre recombination outputs of the hGFAP-dependent Thy1.2-cascade and the Thy1.2-dependent hGFAP-cascade resulted in fluorescent labeling of developmentally distinct cell populations thus confirming the sequential binary recombination mechanism of Co-Driver. With their high activity and fidelity, both Co-Driver and Co-InCre show great potential for robust high-resolution recombination of conditional alleles and lineage-tracing in transgenic mice.

MATERIALS AND METHODS

Construct assembly

All constructs for constitutive mammalian expression were assembled using Golden Gate cloning (19) of PCR products into a pCAG-T7 destination vector. hGFAP and Thy1.2 expression constructs were assembled using standard cloning techniques. All cloning strategies can be provided upon request. Functional plasmids used in this study have been deposited with Addgene and annotated sequences of all plasmids are provided in Supplementary Note 1. hGFAP expression constructs are based on hGFAP-fLuc (20) (Addgene plasmid 40589). Thy1.2 expression constructs are based on Thy1 promoter construct (21) (Addgene plasmid 20736). Codon-optimized SSRs Bxb1, B3 and KD (Genscript) and gp41-1 and DnaE split-inteins (IDT) were gene-synthesized. DreO was a generous gift from C. Monetti. For the construction of Co-InCre expression plasmids, codon-optimized Cre (22) (iCre) was split into a N-terminal (aa 19–59) and a C-terminal (aa 60–343) fragment. Amino acid sequences for gp41-1^{N} and gp41-1^{C} split-intein fragments (16) were back-translated using Emboss Backtranseq (http://www.ebi.ac.uk/Tools/st/emboss_backtranseq/) with mouse codon usage and fused to N- and C-terminal iCre fragments, respectively. The Roxed-Cre expression plasmid was constructed by introducing a rox-flanked STOP cassette [based on the STOP cassette of the CAG-Floxed ZsGreen plasmid (11), Addgene plasmid 22798] in between iCre codons 177 (aa 59) and 180 (aa 60). A single nucleotide (G) was introduced 5′ of the rox-site to create an in-frame insertion of 33 bp into the iCre open reading frame upon Dre recombination.

Animals

Ai6 and Ai14 mice (11) were purchased from Jackson Laboratories, USA, and CD1 mice were purchased from Charles River, Germany. All animals were maintained in temperature- and light-controlled rooms (12 light/12 dark, light on from 6:00 a.m.) with food and water ad libitum.

All experiments including laboratory animals were approved by the Cantonal Veterinary Office of Zurich. The protocol of animal handling and treatment was in accordance with Swiss Federal and Cantonal regulations as well as the internal guidelines of the University of Zurich.

Cell-lines and transfection

Mouse embryonic fibroblast (MEF)-Ai6 were derived from hemizygous Ai6 reporter mice (11) and immortalized using standard methods (23). HEK293T and MEF-Ai6 were transfected in a six well format using XtremeGene 9 (Roche) in a 4:1 transfection reagent/DNA ratio. Individual combinations of recombinase and reporter plasmids were adjusted to a total DNA amount of 1 μg using pUC57 as an inert carrier plasmid. For quantifications, transfections of each distinct combination of plasmids were repeated three times with each replicate experiment including independent DNA preparations for each plasmid, independent transfection reagent/medium preparations and independently seeded cell populations.

Primers

The specific primers used for genotyping of the Ai6 reporter allele (Figure 2D) were Ai6-F, TTTTCCTACA GCTCCTGGGC; Ai6-R, GGCATTAAAGCAGCGTAT CC.

Flow cytometry

HEK293T and MEF-Ai6 cells were trypsinized and collected in PBS with 10% fetal bovine serum 24 and 72 h after transfection, respectively. Cells were analyzed on a BD LSRII Fortessa. ZsGreen fluorescent protein was excited using a 488-nm laser and detected using a 525/50 filter. mCherry fluorescent protein was excited using a 561-nm laser and detected using a 610/20 filter. Single color controls are shown in Supplementary Figure S8. For HEK293T, a minimum of 20 000 and for MEF-Ai6, a minimum of 5000 mCherry-positive events were recorded. Data analysis was performed using FlowJo software, and flow plots were processed using Adobe Illustrator.

In utero electroporation

Uteri of timed-pregnant mothers (CD1, 14.5 days after mating with Ai14-homozygous males) anaesthetized with isoflurane in an oxygen carrier (Merial Animal Health) were exposed through a 2-cm incision in the ventral peritoneum. Embryos were lifted through the incision and placed on humidified gauze pads. DNA (0.5 μg of each recombinase plasmid and 1 μg of EGFP plasmid) was injected through the uterine wall into the telencephalic vesicle using pulled borosilicate needles and a Femtojet microinjector (Eppendorf). Electric pulses were applied using 5 mm platinum tweezers electrodes (CUY650P5, Nepagene) and an ECM-830 BTX square wave electroporator (BTX, Gentronic Inc.). Uterine horns were then placed back into the abdominal cavity, and the abdomen wall and skin were sutured using surgical needle and thread.

Histology and fluorescence imaging

In utero electroporated Ai14-hemizygous mice were sacrificed at P9-10 and perfused with ice-cold 4% PFA in PBS. Brains were harvested and post-fixed in 4% PFA in PBS for at least 4 h on ice. Whole-mount brains were visually inspected using an Olympus SZX12 stereo microscope equipped with epi-fluorescence illumination, and brains with similar-sized areas of EGFP fluorescence were selected for further analyses. About 50–60 μm thick coronal brain sections were prepared using a VT 1000S vibratome (Leica), mounted and imaged using a Fluoview FV10i confocal microscope (Olympus). Images were processed using ImageJ or Imaris (Bitplane Scientific Software), and panels were arranged using Adobe Illustrator.

Quantifications and statistical analysis

Recombination efficiency was determined as the percentage of mCherry-positive cells showing ZsGreen fluorescence. Cre recombination efficiency served as a standard and all replicates were divided by mean Cre recombination efficiency thus transforming data to percentage of Cre recombination efficiency. Standard deviation (SD) was calculated for transformed replicates and is shown as error bars in bar graphs. Two-way ANOVA with Bonferroni *post hoc* test was used to compare multiple means. The number of $EGFP^+$ cells and $tdTomato^+$ cells per coronal brain sections was determined in a single confocal plane and for each fluorescent channel individually using the automatic spot detection function with default parameters (estimated *xy* diameter = 12.4 μm) implemented in Imaris (Bitplane Scientific Software). The spot detection threshold was manually set using the 'quality filter', and detected spots were manually curated to eliminate spots marking false-positive detected cell bodies and add spots for false-negative undetected cell bodies. Based on the proximity of individual spots marking $EGFP^+$ and $tdTomato^+$ cells, respectively, $EGFP^+$ $tdTomato^+$ cells were annotated manually and EGFP/tdTomato co-localization was validated in an overlay image of the green and red fluorescence channels (the workflow is outline in Supplementary Figure S9). Average numbers of cells were calculated for three mice per group and three coronal sections per mouse. Student's *t*-test (two-tailed) was used to compare two means. For all statistical analyses, a *P*-value of <0.05 was considered significant.

RESULTS

Dre as the optimal Co-Driver recombinase

The basic concept of the Co-Driver cascade requires the use of a highly active SSR that will operate orthogonally with Cre. We considered SSRs to be promising Co-Driver candidates if they fulfilled two essential conditions. First, the specificity of the SSRs for their cognate recognition

sites (and the absence of cross reactivity with other SSR recognition sites) should have been determined previously and preferentially also validated in a mammalian system. Second, the Co-Driver candidate and its recognition sites should not be routinely utilized for cloning or recombineering of transgenic constructs. Selecting SSRs by these criteria should minimize the risk of unintended recombination events when Co-Driver is combined with currently available transgenic alleles. Following these considerations, we selected four Co-Driver candidates including the phage recombinases Dre (13,14) and Bxb1 (24–26) as well as the yeast recombinases B3 and KD (27). We excluded the extensively characterized SSRs Flp and PhiC31 since a large number of established mouse lines carry conditional mutagenesis cassettes, which already contain *frt* and PhiC31 *attB*/*attP* recognition sites (11,12).

To date, no comparative assessment of recombination efficiency of these SSRs has been performed in a standardized mammalian system. We therefore systematically compared their recombination efficiencies relative to the highly active Cre recombinase. First, we generated standardized SSR overexpression constructs by fusing all the codon-optimized SSR protein-coding sequences to an N-terminal SV40-NLS and a HA-tag to and placing them under control of a constitutively active CAG promoter (Figure 1A). B3, KD and Dre are members of the tyrosine SSR family, whereas Bxb1 is the only representative of the serine family of recombinases. The recombination mechanism of tyrosine family SSRs in combination with their native recognition sites typically favors excision over insertion reactions, while inversions of DNA are generally reversible as long as the SSR is present. Serine

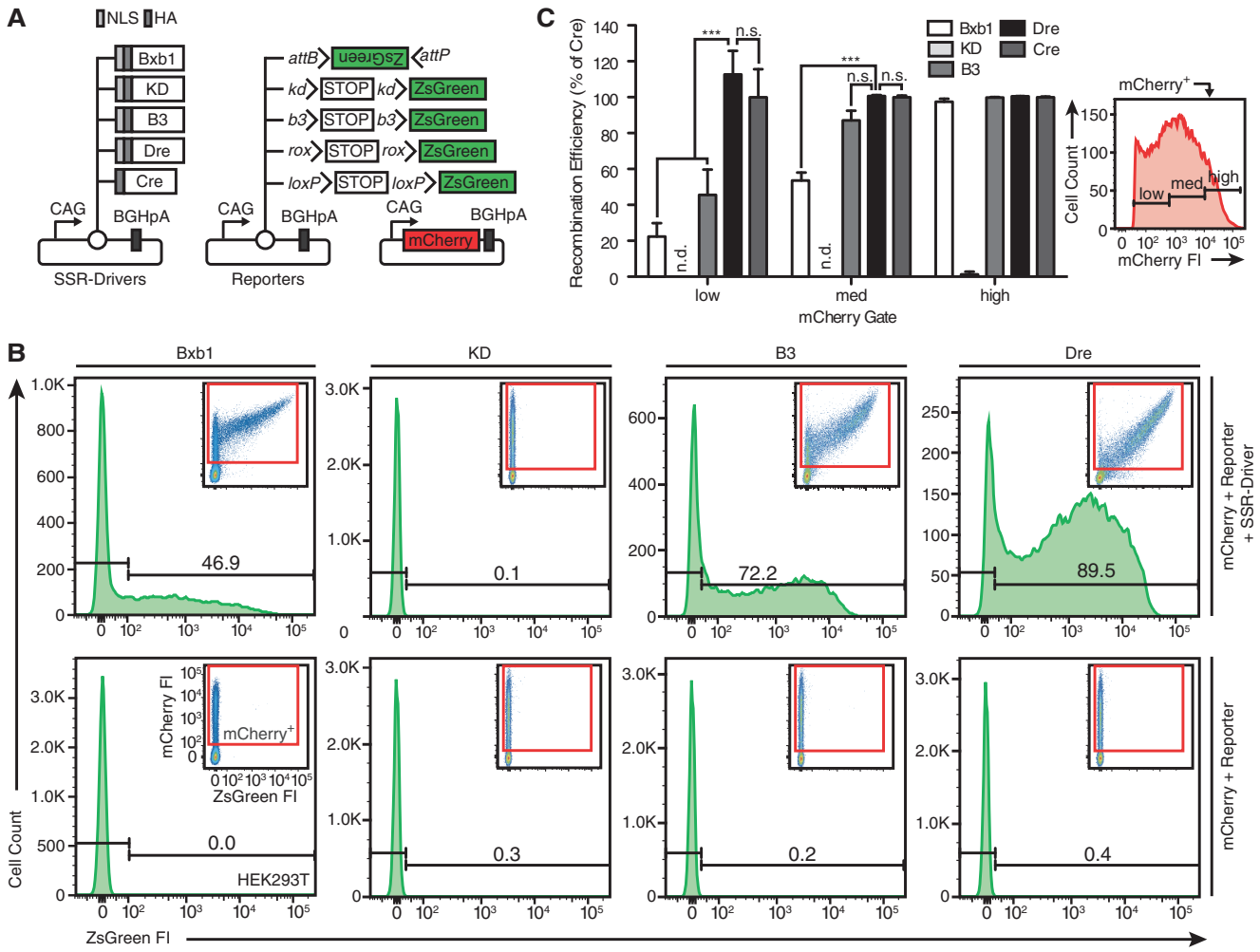

Figure 1. Evaluation of Co-Driver candidate recombinases. **(A)** Diagrams of standardized SSR-driver and respective reporter plasmids that are co-transfected with a constitutively expressing mCherry plasmid into HEK293T cells. Transfected cells are mCherry$^+$, and SSR activity is detected for Bxb1 using an inverted ZsGreen reporter or a STOP-cassette-based ZsGreen reporter for KD, B3 and Dre. Arrowheads indicate the orientation of individual SSR recognition sites. **(B)** Flow cytometric analysis of cells 24 h after transfection with Bxb1, KD, B3 or Dre recombinase and respective reporter constructs (top panels) or reporter constructs alone (bottom panels). Numbers within histograms represent the percentage of transfected cells showing recombination activity. Insets, scatter plots showing living cells and gating for mCherry$^+$ cells (red rectangle). FI, relative fluorescence intensities reported in arbitrary units. **(C)** Quantification of recombination efficiency for Co-Driver candidates. Bars represent the percentage of cells showing recombination activity in subsets of mCherry$^+$ cells [low, medium (med) or high mCherry expression; gating within the mCherry$^+$ gate is shown right to bar graph]. Average data of three independent experiments with standard deviation and normalized to 100% Cre average recombination efficiency are shown. KD activity was not detectable (n.d.) in mCherry$^+$ cells except in the mCherry^{high} population. Statistics: two-way ANOVA with Bonferroni *post hoc* test; n.s., not significant; $*P < 0.05$; $**P < 0.01$; $***P < 0.001$.

family SSRs such as Bxb1, on the other hand, are capable of carrying out unidirectional excisions and inversions (28). As our intent was to exploit the DNA inversion mechanism of Bxb1 to construct a Bxb1/Cre SSR cascade, we assessed the efficiency of Bxb1 in the context of a fluorescent reporter construct carrying a reverse-complementary ZsGreen protein-coding sequence flanked by Bxb1 recognition sites (Figure 1A). Conversely, the DNA excision activity of the three tyrosine recombinases was assessed using reporter constructs carrying ZsGreen preceded by a STOP-cassette flanked by the cognate recognition sites of the respective SSR.

To ascertain SSR activity, we co-transfected HEK293T cells with a constitutively expressing mCherry plasmid, SSR drivers and their respective reporters and measured single-cell mCherry and ZsGreen fluorescence intensities using flow cytometry (Figure 1B). In the absence of SSRs none of the reporter constructs produced any ZsGreen signal detectable by fluorescence microscopy (Supplementary Figure S1) and flow cytometric analysis 24 h post-transfection revealed background ZsGreen fluorescence in <0.5% of cells (Figure 1B). We defined recombination efficiency as percentage of transfected ($mCherry^+$) cells showing ZsGreen expression as a result of SSR activity. To determine recombination efficiencies in subsets of cells with overall low, medium and high expression levels we defined three equally sized gates within the $mCherry^+$ gate covering the full range of mCherry fluorescence intensities (Figure 1C). Dre recombination levels were comparable to Cre in all sub-populations including $mCherry^{low}$ cells, while B3 reached only 50% of Cre activity in this population. We could not detect any KD recombination events above background levels in this experiment, however, a KD variant with C-terminal fusion of a PEST sequence (27) showed residual activity 72 h post-transfection (data not shown). Bxb1-mediated inversion of the ZsGreen reporter was only 20% as efficient than Cre-mediated STOP-cassette excision in $mCherry^{low}$ cells.

These results prompted us to consider Dre as the optimal Co-Driver of all SSR tested for constructing a sequential binary recombinase system.

A Dre-responsive Cre driver design

Having selected Dre as the Co-Driver SSR, we evaluated several rox-flanked STOP-cassette designs with the aim to tightly control Cre expression in the absence of Dre. We adapted two STOP-cassette configurations that were shown previously to completely block transgene expression and at the same time facilitated efficient transgene reactivation upon the removal of the STOP cassette by Cre recombination. The 3× poly(A) STOP cassette incorporates STOP codons in all three reading frames followed by three consecutive SV40 poly(A) sequences and is part of the Ai6 and Ai14 conditional reporter alleles (11). The chloramphenicol acetyltransferase (CAT)-poly(A) STOP cassette is composed of a CAG promoter, the CAT gene and a poly(A) signal and has been shown to tightly control multi-copy transgenes (29). We cloned both rox-flanked STOP-cassettes upstream of *Cre* (Figure 2A) and transfected HEK293T cells with each of these constructs together with constitutive mCherry plasmid, Cre-inducible ZsGreen reporter and either adding or omitting a constitutive Dre expression construct (Figure 2B). We observed substantial levels of *loxP*-recombination events in the absence of Dre regardless of which *rox*-flanked STOP cassette was present upstream of *Cre* (Figure 2B and C; Supplementary Figure S2). Similar amounts of leakage were detected, when *Cre* was preceded by a *b3*- or *kd*-flanked STOP cassette (data not shown). We hypothesized that the poly(A) signals of the upstream STOP cassettes allow sufficient transcriptional read-through for translation of *Cre* and subsequent *loxP*-recombination to occur. Therefore, we devised a strategy that would interrupt Cre expression at both the transcriptional and translational level. In the Roxed-Cre construct (Figure 2A), the *Cre* open reading frame is interrupted by the 3× poly(A) STOP cassette between amino acids 59 and 60. Thus, Roxed-Cre generates an inactive N-terminal Cre fragment (5–9) in the absence of Dre recombination (and in the case of transcriptional read-through the also inactive C-terminal Cre fragment). Once the rox-flanked STOP cassette is removed a Cre variant with an 11 amino acid insertion resulting from translation of the remaining rox-site is expressed (Supplementary Figure S4). Roxed-Cre reduced unintended *loxP*-recombination below detectable levels in all $mCherry^+$ cells, while appearing to be equally efficient as Cre when Dre was added to Roxed-Cre transfections (Figure 2B and C).

Co-Driver recombination of a genomic single-copy reporter gene

In transgenic mice, Cre is typically employed to recombine hemizygous reporter genes or homozygous loxP-flanked conditional alleles. It has been shown that while Cre maintains high activity on both plasmid-based and chromatin targets other recombinase systems such as FLP/frt are significantly less efficient in processing the latter (30). To assess Co-Driver performance in an experimental environment that closely resembles *in vivo* conditions we established a MEF cell line that carries a single-copy Cre-inducible ZsGreen reporter [MEF-Ai6 derived from hemizygous Ai6 mice (11), Figure 2D]. MEF-Ai6 displayed green fluorescence with uniform intensity 72 h after Cre transfection (Figure 2D) as expected for a *ROSA26*-targeted reporter (31). We transfected MEF-Ai6 with either single or both components of Co-Driver together with a mCherry construct and assessed recombination events 72 h after transfection. The correct processing of the Ai6 allele was clearly evidenced by PCR analysis (Figure 2D) and ZsGreen fluorescence (Figure 2E; Supplementary Figure S3) in MEF-Ai6 transfected with both components, while no recombination was observed in single component transfections.

Having confirmed that both Co-Driver components are essential for processing a single-copy Cre-dependent reporter gene we went on to evaluate the performance of Co-Driver in relation to Cre and other binary SSR systems. We first asked how efficiently the Cre variant

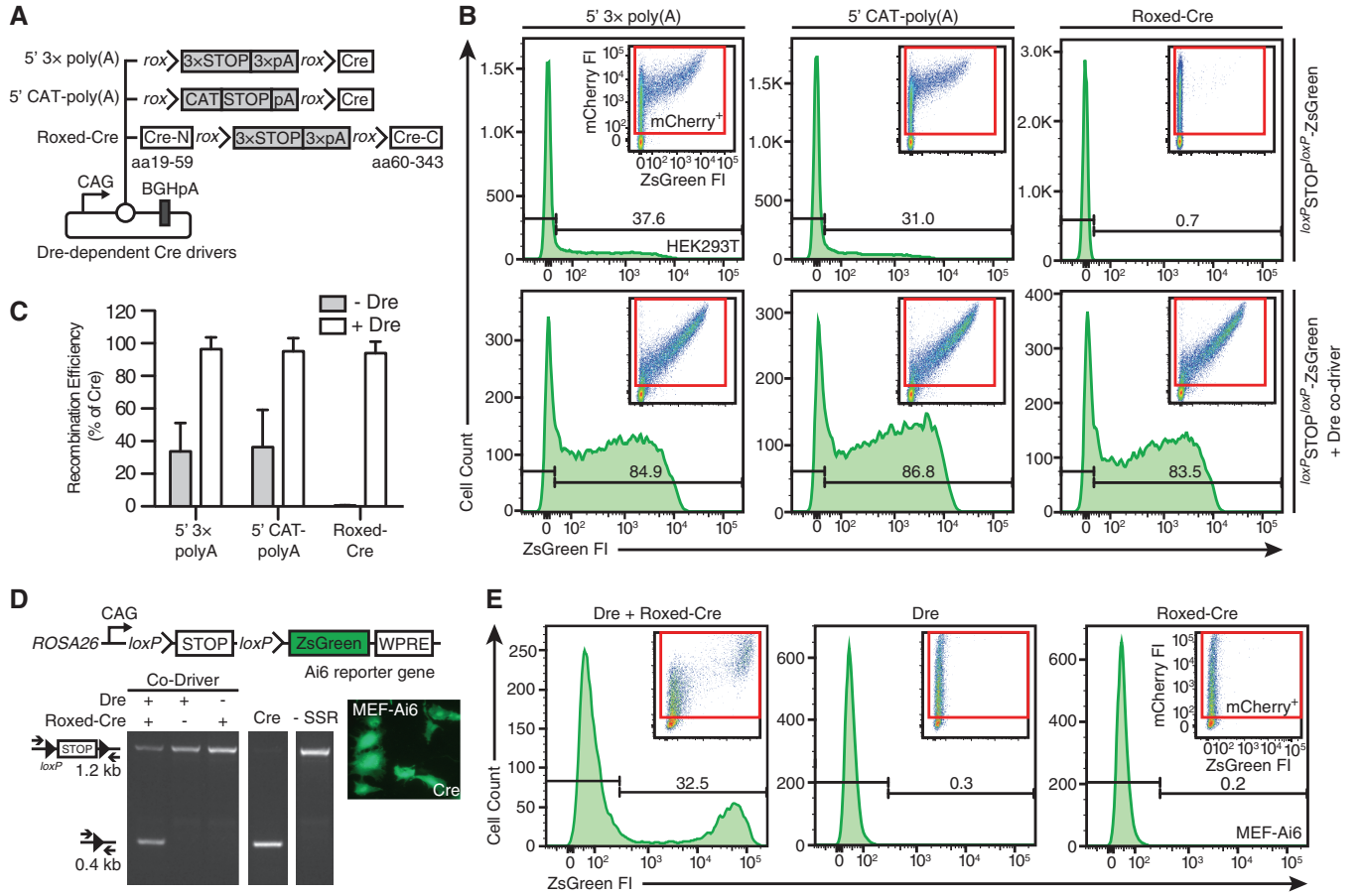

Figure 2. Dre-dependent activation of Cre. **(A)** Diagram depicting Dre-dependent Cre driver candidates 5′ 3× poly(A), 5′ CAT-poly(A) and Roxed-Cre with distinct rox-flanked STOP cassette configurations. In the case of Roxed-Cre, the Cre protein-coding sequence is interrupted by a rox-flanked STOP cassette inserted in between the codons of amino acids (aa) 59 and 60. **(B)** Activity of Cre driver candidates in transfected (mCherry^{+}) HEK293T is detected using a ZsGreen reporter plasmid. Representative flow plots 24 h after transfection of HEK293T cells with a loxP-flanked ZsGreen reporter, Cre-Driver candidates and either omitting (top row) or adding (bottom row) Dre. **(C)** Quantification of recombination activity of Cre driver candidates with or without Dre Co-Driver. Bars represent the percentage of transfected cells showing recombination activity. Average data of three independent experiments are shown with standard deviation and normalized to 100% Cre average recombination efficiency. **(D)** MEFs derived from hemizygous Ai6 reporter mice (MEF-Ai6) express ZsGreen from the single copy Ai6 transgene (D top panel; WPRE, woodchuck hepatitis virus post-transcriptional regulatory element) upon Cre recombination (D right panel; fluorescence microscopic image of MEF-Ai6 72 h after transfection with Cre). Combined, but not single transfections of Co-Driver modules Dre and Roxed-Cre result in excision of the loxP-flanked Ai6 STOP cassette, as detected by the presence of a 0.4-kb PCR fragment using primers located upstream and downstream of the STOP cassette (D bottom panel) and expression of ZsGreen, as detected by flow cytometry **(E)** in MEF-Ai6 72 h post-transfection.

translated from Dre-processed Roxed-Cre (Cre$^{Rox60\text{-}70}$, Figure 3A; Supplementary Figure S4) would recombine the Ai6 reporter. In transfected MEF-Ai6, Cre$^{Rox60\text{-}70}$ (expressed from a construct mimicking complete processing of Roxed-Cre plasmids by Dre) showed a 30–40% lower recombination activity than native Cre (Supplementary Figure S4). Since Cre$^{Rox60\text{-}70}$ seems to be a limiting factor for overall Co-Driver recombination efficiency, we explored a different sequential binary SSR configuration that could generate native Cre as a final output. We flanked the reverse complementary Cre protein-coding sequence (rcCre) by Bxb1 recognitions sites, *attB* and *attP*, in inverted orientation (Figure 3A). Thus, expression of Bxb1 will restore the correct orientation of the Cre open reading frame by unidirectional inversion.

Besides our attempts to identify the optimal sequential binary SSR configuration we were also interested in constructing a coincidental binary SSR that allows seamless reconstitution of native Cre. Here, we capitalized on the recently described gp41-1 split-intein (15,16) to construct Co-InCre (Figure 3B; Supplementary Figure S5), a coincidental binary SSR akin to the previously described split-intein-split-Cre (9). gp41-1 exhibits the highest trans-splicing activity at 37°C of all split-inteins described to date and does not require any native extein sequences to catalyze this reaction (15). We cloned Co-InCre as well as the previously published Split-Cre (6) and split-intein-split-Cre (9) into our standard expression vector and compared their recombination efficiency to Co-Driver, Bxb1-rcCre and native Cre in transfected MEF-Ai6 (Figure 3C). Again, we used flow cytometry to analyze subsets of mCherry^{+} MEF-Ai6 with low, medium and high mCherry fluorescent intensities (Figure 3D).

Not surprisingly, none of the binary SSRs reached the recombination efficiency of Cre in mCherry^{low} or mCherry^{med} cell populations, however, there were

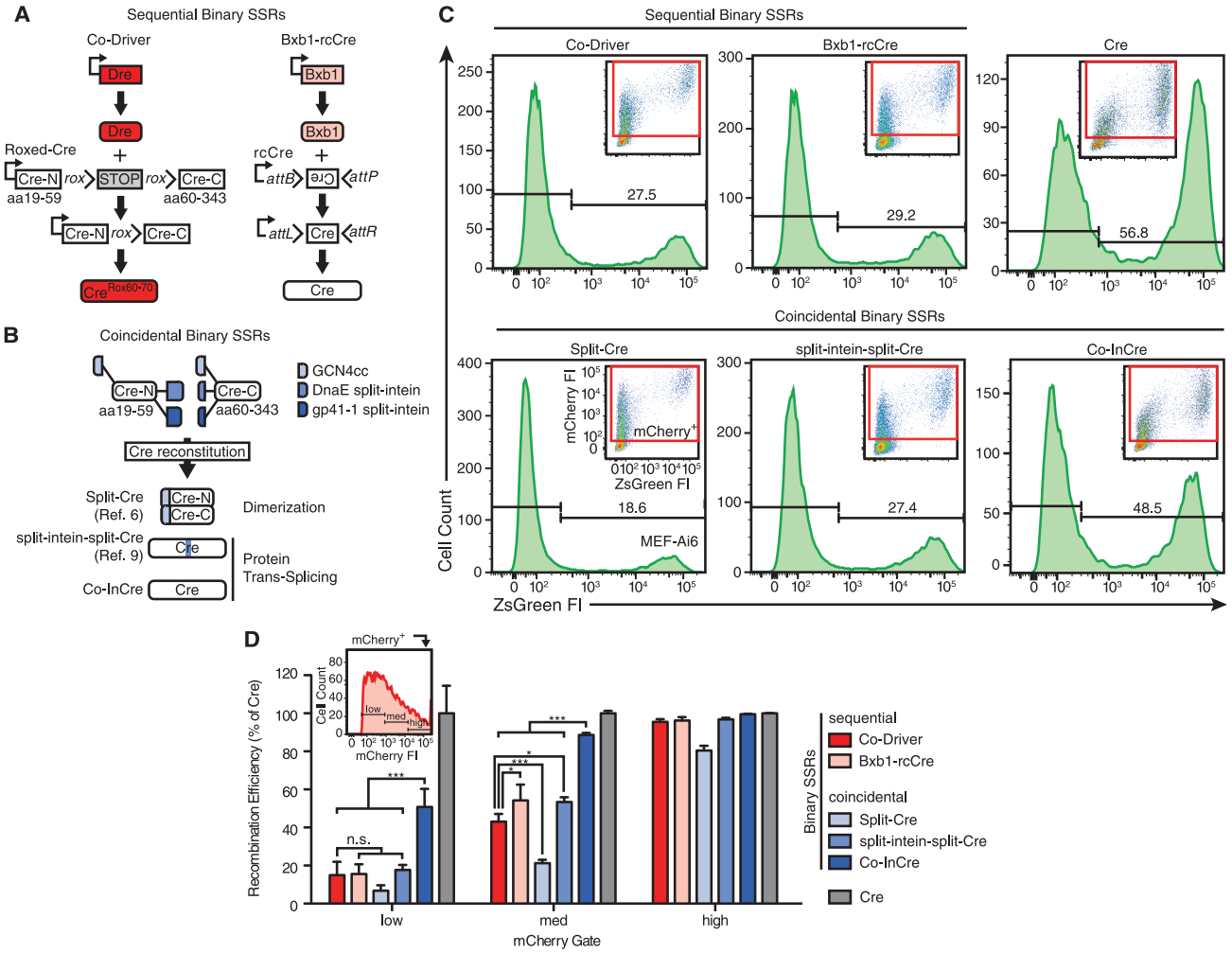

Figure 3. Recombination efficiency of Co-Driver and Co-InCre. **(A)** Sequential binary SSRs Co-Driver and Bxb1-rcCre comprise expression constructs for the primary recombinases Dre and Bxb1, which subsequently activate expression of functional Cre by removal of a rox-flanked STOP cassette or by inversion of attB/attP-flanked reverse complement (rc) Cre, respectively. Rectangles with arrows represent expression constructs and rounded rectangles represent proteins. **(B)** Coincidental binary SSRs generate active Cre from split-proteins (Cre-N, aa 19–59; Cre-C, aa 60–343; white rectangles) fused to protein reconstitution domains (blue rounded rectangles) by GCN4-coiled-coil (cc)-mediated dimerization [Split Cre (6)], DnaE-mediated protein trans-splicing yielding Cre with inserted non-native amino acids [split-intein-split-Cre, (9)] and Co-InCre reconstituting native Cre by gp41-1-mediated seamless protein trans-splicing. **(C)** MEF-Ai6 were transfected with a plasmid for constitutive mCherry expression and either two plasmids for the expression of both binary SSR modules or a single Cre plasmid. Representative flow plots 72 h post-transfection show the percentage of transfected cells with recombination activity for sequential binary SSRs and Cre (top) and coincidental binary SSRs (bottom). Transfected binary SSR systems are indicated on top of the flow plots. Insets show gating for transfected cells. **(D)** Recombination efficiency, defined as ratio of mCherry$^+$ cells showing ZsGreen-expression, was determined in subsets of mCherry$^+$ cells with low, medium (med) or high mCherry FI (gating within the mCherry$^+$ gate is shown in the graph). Binary SSRs with sequential or coincidental mode of action are color-coded in shades of red, or blue, respectively. Average data of three independent experiments are shown with standard deviation and normalized to 100% Cre recombination efficiency. Statistics: two-way ANOVA with Bonferroni *post hoc* test; n.s., not significant; $*P < 0.05$; $**P < 0.01$; $***P < 0.001$.

significant differences in performance between the individual systems (Figure 3D). In mCherry^{low} cells, Co-Driver and Bxb1-rcCre showed ~20% of Cre efficiency, which was similar to split-intein-split-Cre and slightly above Split-Cre. Remarkably, Co-InCre was more than twice as active as any other binary SSR reaching more than 50% of Cre efficiency. Co-InCre also showed the highest performance in mCherry^{med} cells with ~80% of Cre efficiency. Here, Co-Driver activity was superior to Split-Cre, while being slightly lower than Bxb1-Cre^{rc} and split-intein-split-Cre. Thus, a considerable gain in efficiency at low expression levels could be achieved by the seamless protein trans-splicing of Co-InCre. Bxb1-rcCre, on the other hand, only permitted an increased SSR activity relative to Co-Driver in cells with higher expression levels.

Co-Driver and Co-InCre recombination in the developing mouse brain

The utility of SSRs for *in vivo* conditional transgenesis depends on their functionality within rapidly changing cellular environments during organogenesis or differentiation processes on-going during adulthood. In the developing mouse neocortex, heterogeneous populations of progenitor cells residing in the ventricular zone (VZ) and the subventricular zone start to produce neurons around

embryonic day (E) 10.5. Corticogenesis proceeds in an 'inside-out' fashion, i.e. neocortical layer VI is established first, followed by layers V, IV and lastly layers II/III (32). After neurogenesis is completed around E16.5, progenitors start to generate astrocytes and oligodendrocytes (32,33). Between E12.5 and E16.5, VZ progenitor cells can be transiently transfected using *in utero* electroporation of mouse embryos (34,35). Here, progenitors receive a limited number of plasmid copies, which, upon cell division, are inherited by daughter cells. While gene expression from introduced plasmid DNA is remarkably stable in post-mitotic cells, it is rapidly lost in dividing progenitors, probably due to the successive loss of the extrachromosomal plasmids with each cell division. Therefore, those neural cells born shortly after electroporation will show the highest level of transgene expression, while those born later only show low levels or no expression at all. Neurons born before the time point of electroporation will not receive any plasmid DNA and as a consequence will not express the transgene. Depending on the embryonic stage at which electroporation is performed the progeny of the transfected progenitors will populate specific cortical layers and express one or multiple introduced transgenes in the adult brain (34–36).

To evaluate the full recombination potential of our binary SSRs *in vivo*, we electroporated CAG-driven Co-Driver or Co-InCre plasmids together with a CAG-driven EGFP plasmid into the embryonic (E14.5) brains of Ai14 tdTomato reporter mice (11) (Figure 4A). We identified electroporation-positive brain areas in post-natal mice (P9-P10, Figure 4B) and imaged coronal brain sections for $EGFP^+$ and $tdTomato^+$ cells using confocal microscopy (Figure 4C–F). Confirming our previous observations in transfected MEF-Ai6 cells, single Co-Driver (Figure 4C) and Co-InCre (Figure 4E) modules did not trigger any detectable tdTomato expression over a time period of more than 2 weeks following electroporation. Brains of mice electroporated with binary Co-Driver or Co-InCre showed extensive tdTomato-fluorescence in the electroporated hemispheres with the vast majority of positive cells being found in upper cortical layers (Figure 4C and E). High magnification images revealed that tdTomato-positive cells substantially outnumbered those that were EGFP-positive (Figure 4D) indicating that cells, which had received lower amounts of plasmid and therefore could not produce detectable amounts of EGFP, were nevertheless able to produce amounts of Cre that were sufficient for the processing of the Ai14 reporter gene. In all mice analyzed, gross morphology of the cortex appeared normal. Fluorescently labeled neurons projected locally to neurons of deeper cortical layers as well as through the corpus callosum (Figure 4D) toward distal regions in the contralateral hemisphere. Thus, Co-Driver and Co-InCre activity was well tolerated by neuronal populations and their precursor cells in the developing mouse brain.

Sequential expression of Co-Driver modules in the mouse neocortex

In a final series of experiments, we asked whether we could manipulate the output of Co-Driver, i.e. the timing and cell-type specificity of Cre recombination, by producing Dre and Roxed-Cre from distinct tissue-specific expression constructs. To address this question, we cloned Dre and Roxed-Cre into a hGFAP-promoter (17) cassette and the Thy1.2 expression cassette (18) to generate hGFAP-Dre, hGFAP-Roxed-Cre, Thy1.2-Dre and Thy1.2-Roxed-Cre constructs [Figure 5A, here, Dre was fused to the porcine teschovirus-1 (P)2 A sequence (37) and the blue fluorescent protein, mTagBFP (38)]. hGFAP-Cre transgenic mice express Cre in radial glia, the principal VZ precursor cells, between E13 and E17 and in the adult brain in astrocytes but not in neurons or oligodendrocytes (39). Since radial glia give rise to neurons, astrocytes and oligodendrocytes, activation of a Cre-dependent reporter allele in radial glia results in labeling of all three cell lineages in the adult brain.

In the post-natal mouse neocortex, Thy1.2-driven fluorescent proteins can be detected in neurons throughout cortical layers II–VI (21) and two lines of Thy1.2-brainbow mice showed expression in astrocytes (40). For a large number of transgenic lines, Thy1.2-driven transgenes have been reported to reach detectable expression levels in the post-natal brain (18,21,41). However, several lines of Thy1.2-Cre mice already showed reporter gene activation during embryonic development (42).

First, we assessed the expression profiles of single Thy1.2- and hGFAP-driven Roxed-Cre plasmids by combining each of them with the continuously expressing CAG-Dre construct (Supplementary Figure S7). In the post-natal brains of Ai14 mice that were electroporated at E14.5 with CAG-Dre, Thy1.2-Roxed-Cre and CAG-EGFP, recombination was restricted to $NeuN^+$ cortical neurons, which typically also exhibited EGFP fluorescence (Supplementary Figure S7A). Combining CAG-Dre with hGFAP-Roxed-Cre resulted in a more extensive pattern of recombination within and beyond the area of $EGFP^+$ cells. Here, we observed tdTomato-labeling of $NeuN^+$ neurons and $NeuN^-$ cells morphologically resembling astrocytes in the cortex and $tdTomato^+$ $NeuN^-$ cells in proximity of the corpus callosum (Supplementary Figure S7B).

We then introduced the Co-Driver pairs, hGFAP-Dre with Thy1.2-Roxed-Cre (hGFAP→Thy1.2) and Thy1.2-Dre with hGFAP-Roxed-Cre (Thy1.2→hGFAP), into the embryonic mouse brain. Confocal imaging of post-natal coronal brain sections consistently showed reporter gene activation by both Co-Driver pairs. However, there was a remarkable difference in the lineage identity and radial positions of $tdTomato^+$ cells relative to $EGFP^+$ cells for hGFAP→Thy1.2 and Thy1.2→hGFAP electroporations, respectively (Figure 5B). In hGFAP→Thy1.2-electroporated brains the vast majority of $tdTomato^+$ cells stained positive for NeuN (Supplementary Figure S8) and large numbers of these neurons either showed EGFP fluorescence themselves or occupied similar radial positions relative to their $EGFP^+$ neighbors. Thy1.2→hGFAP, on the other hand, targeted tdTomato expression predominantly to $EGFP^-$ cells with $tdTomato^+$ $NeuN^+$ neurons occupying positions closer to the pial surface and $tdTomato^+$ $NeuN^-$ non-neuronal cells residing also in lower cortical layers and in the white

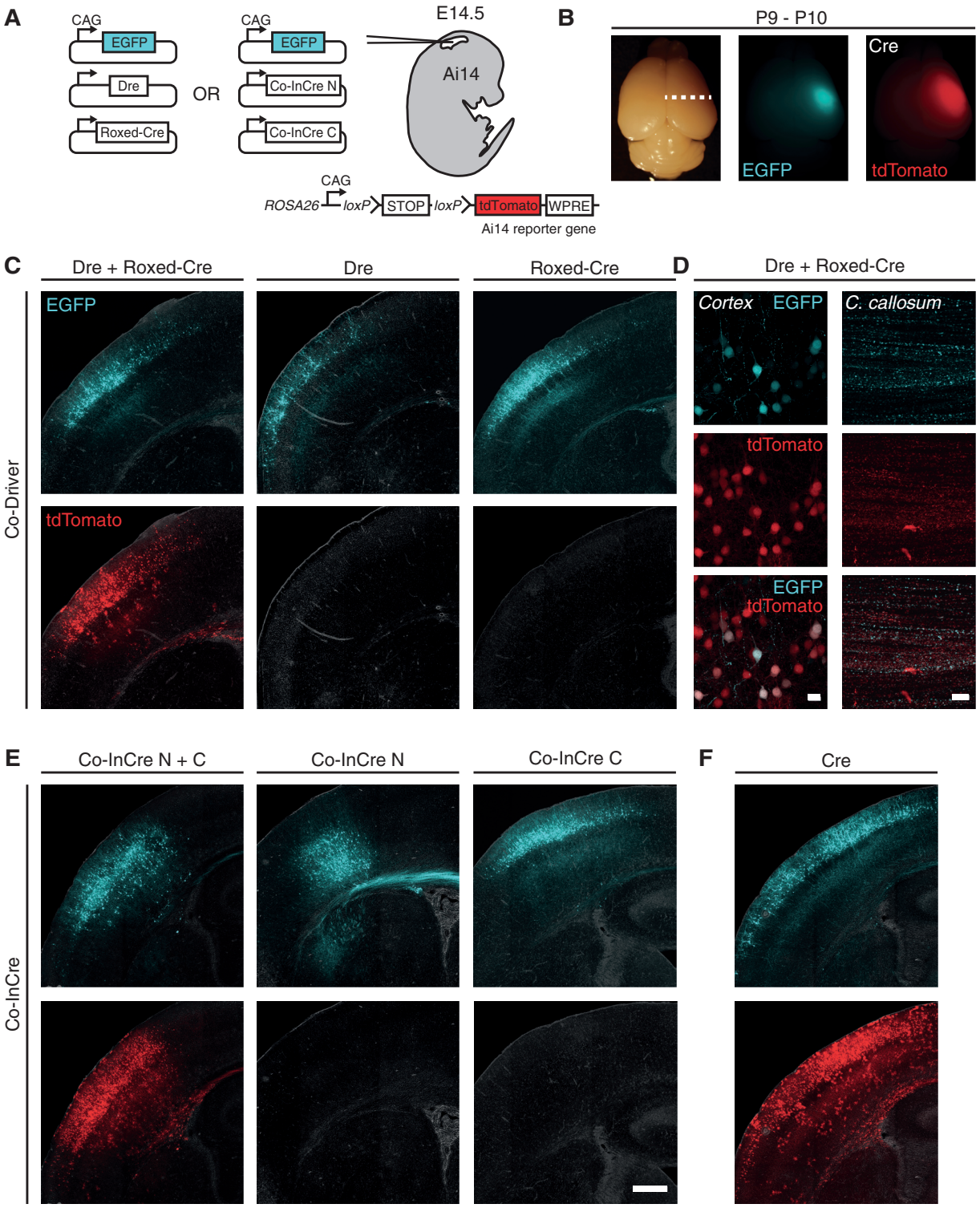

Figure 4. Co-Driver and Co-InCre trigger efficient recombination in the developing mouse brain. **(A)** A constitutively expressing EGFP plasmid and plasmids encoding either the Co-Driver or the Co-InCre components were electroporated into the developing brains of embryonic day 14.5 (E14.5) hemizygous Ai14 reporter mice. Upon Cre recombination, these mice express tdTomato from a single reporter gene integrated into the *ROSA26* locus (WPRE). **(B)** Coronal sections of fluorescence-positive brain areas (white dashed line) were prepared from post-natal Day 9–10 (P9–P10) mice. The post-natal brain of an animal electroporated with EGFP and Cre plasmids is shown. **(C–F)** Maximum intensity projections (MIP) of electroporation-positive brain areas (coronal brain sections). (C) Cre-induced tdTomato expression can only be detected by confocal imaging when both Co-Driver components, Dre and Roxed-Cre, were electroporated. Fluorescent signals are combined with phase-contrast images of brain sections. (D) High magnification MIP of recombination-positive areas in the cortex (left) and long-range axonal projections in the corpus (c.) callosum (right). (E) Both Co-InCre N- and C-terminal fragment evoke recombination in electroporation-positive areas, while single components show no recombinase activity. (F) Control electroporation using full-length Cre recombinase. Scale bar for panels (C), (E) and (F), 500 μm. Scale bars for panel (D), 20 μm.

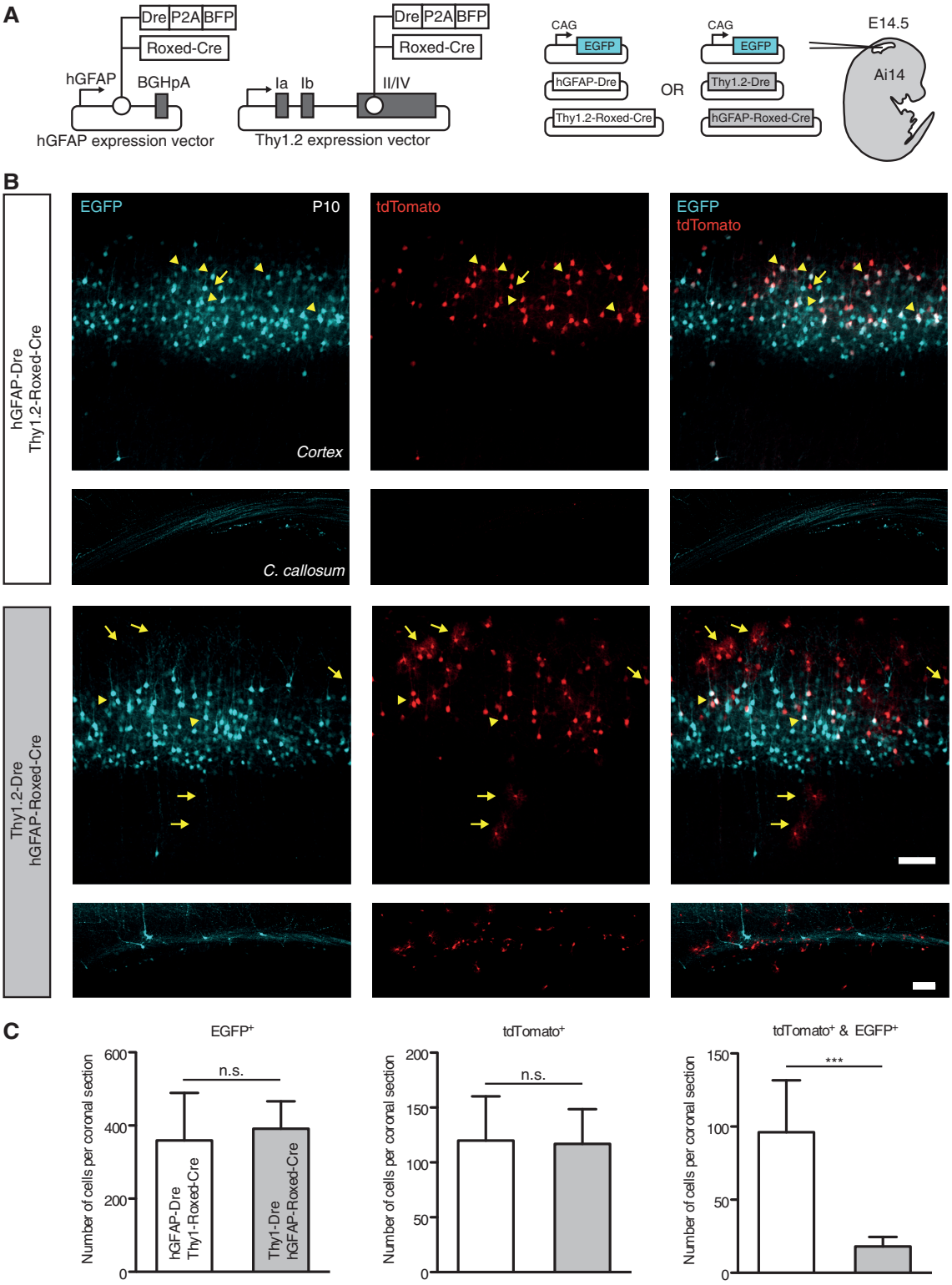

Figure 5. Sequential expression of Co-Driver components during development of the mouse neocortex. **(A)** Co-Driver components Dre [fused to the porcine teschovirus-1 (P)2A sequence and blue fluorescent protein, BFP] and Roxed-Cre were introduced into a human (h)GFAP promoter expression vector and the Thy1.2 expression vector. E14.5 embryos carrying a single-copy Cre-inducible tdTomato reporter gene (Ai14) were electroporated with a constitutively expressing EGFP plasmid and either hGFAP-Dre with Thy1.2-Roxed-Cre (white rectangles) or Thy1.2-Dre with hGFAP-Roxed-Cre (gray rectangles). **(B)** Representative single-plane confocal images of fluorescence-positive areas within the cortex and MIP of areas in proximity to the corpus (c.) callosum of post-natal day (P)10 mice are shown (top panel, hGFAP-Dre with Thy1.2-Roxed-Cre electroporations; bottom panel, Thy1.2-Dre with hGFAP-Roxed-Cre electroporations). Arrow heads denote cells within the cortex that show both EGFP and tdTomato fluorescence, arrows denote cells with single tdTomato fluorescence. Scale bars, 100 µm. **(C)** Quantification of EGFP-positive cells (left), tdTomato-positive cells (middle) and tdTomato/EGFP double-positive cells (right) in coronal brain sections. Average data of three animals and three coronal sections per animal with standard deviation are shown. Statistics: unpaired Student's *t*-test; $***P < 0.001$.

matter proximal to EGFP$^+$ fibers of callosal projection neurons (Figure 5B; Supplementary Figure S8). While both hGFAP- and Thy1.2-constructs seemed to reliably produce sufficient amounts of Dre we were unable to detect BFP fluorescence in post-natal brains (data not shown) indicating that at the time of analysis the respective activity of neither promoter was sufficient to generate detectable amounts of BFP.

To substantiate the qualitative assessment of Cre recombination patterns, we quantified the numbers of EGFP$^+$ cells, tdTomato$^+$ cells and EGFP$^+$ tdTomato$^+$ cells in electroporation-positive coronal brain sections that were randomly selected along the rostral-caudal brain axis (three brains for each Co-Driver pair with three sections per brain, Figure 5C). Cell counts per coronal section were similar for EGFP$^+$ cells (hGFAP→Thy1.2, 359 ± 130 and Thy1.2→hGFAP, 391 ± 75) and tdTomato$^+$ (120 ± 40 and 117 ± 32), while there was a significantly higher number of cells showing cytoplasmic co-localization of EGFP and tdTomato in hGFAP→Thy1.2 brain sections (96 ± 36 and 18 ± 7). Considering that expression of detectable levels of EGFP is restricted to cells born shortly after *in utero* electroporation was performed (36) these observations suggest that the Thy1.2→hGFAP Co-Driver pair targeted reporter gene activation mainly to cells that were born later relative to the tdTomato$^+$ cells observed as a result of hGFAP→Thy1.2 Co-Driver activity.

DISCUSSION

The principal aim of this study was to design and validate binary SSR systems that can integrate the transcriptional profiles of a wide range of promoters and thus hold the potential to significantly increase the resolution of genetic lineage tracing. Co-Driver demonstrates for the first time the implementation of the sequential lineage tracing concept by using a cascade of two orthogonally active SSRs, which we termed sequential binary SSR. This concept relies on exploiting the temporal activity profiles of two individual promoters to create a genetic record in a distinct sub-population of a cell lineage. The generation of a high fidelity binary SSR system requires the design of two modules that can only produce the desired output in combination but not individually. We challenged the individual Co-Driver modules Dre and Roxed-Cre in several biological systems such as transfected cell lines with plasmid-based or chromosomal Cre-dependent fluorescent reporters and in the developing brains of Cre reporter mice without detecting any spurious recombination events caused by either Dre or Roxed-Cre. Thus, Co-Driver is essentially an obligate binary SSR, with production of functional Dre solely depending on the expression profile of the Dre-driving promoter, while active Cre is only produced when two conditions are fulfilled, (i) the Roxed-Cre gene has been processed by Dre and (ii) the Roxed-Cre-driving promoter is transcriptionally active.

Tissue-specific promoters and expression cassettes harbor regulatory elements that exercise control over the cell-type specificity as well as the timing of gene expression. We could show that Co-Driver integrates both tissue-specific and temporal layers of control when Dre and Roxed-Cre are expressed from two promoters with non-identical transcriptional profiles. This directional mechanism of integrating transcriptional activities of two individual promoters was evident in the developing mouse neocortex. Here, the combination of hGFAP and Thy1.2 expression constructs targeted activation of a Cre reporter gene to distinct cell populations depending on which expression construct harbored Dre or Roxed-Cre, respectively. While hGFAP-dependent Thy1.2-Roxed-Cre expression restricted reporter gene expression to neurons that were born shortly after these constructs were introduced into precursors by *in utero* electroporation, Thy1.2-dependent hGFAP-Roxed-Cre expression resulted in reporter gene activation in later-born neurons as well as cells of the glial lineages.

Conceptually, sequential linage tracing approaches can be performed using different classes of promoter pairs to control the Co-Driver modules including temporally non-overlapping promoter pairs (Figure 6A and B) and promoters that are both active during a certain period of time (Figure 6C–E). For two hypothetical promoters with no temporal overlap in their transcriptional activities, only the early expression of Dre (Figure 6A) but not the early expression of Roxed-Cre (Figure 6B) will result in processing of a loxP-flanked sequence (coincidental binary SSRs cannot produce functional Cre in both scenarios). Conversely, any form of temporal overlap between two promoters should facilitate efficient Co-Driver functionality akin to coincidental binary SSRs such as Co-InCre and earlier published systems (Figure 6C–E).

In terms of versatility, Co-Driver combines the advantages of two classes of previously published binary SSR systems. Co-Driver relies exclusively on Cre-dependent alleles to generate a binary output akin to Cre reconstitution systems (6,9) thus making it compatible with a plethora of available Cre reporter lines (11,31,40,43), diphtheria toxin-based responder mice for conditional cell ablation (44,45) and mice that harbor conditional knockout alleles (12). However, unlike these complementation systems that function best when similar amounts of the two inactive Cre precursor polypeptides are expressed, the Co-Driver cascade of two highly active SSRs should better tolerate a mismatch of transcriptional levels between the two driving promoters in a manner similar to Cre/Flp systems (10). Conversely, the Cre/Flp approach facilitates intersectional labeling of cells but relies on purpose-designed dual-stop-cassette reporters and thus cannot be combined with currently available Cre-responsive alleles.

In addition to Co-Driver, we have characterized two alternative obligate binary SSR systems. First, a binary SSR cascade could also be constructed using the alternative SSR pair Bxb1/Cre, which generates native Cre recombinase upon Bxb1-mediated inversion of a reverse-complementary Cre expression cassette. Thus, we provide evidence that construction of sequential binary SSRs is a generally applicable concept for potentially any combination of SSRs, which exhibit high individual recombination efficiencies and do not cross-react

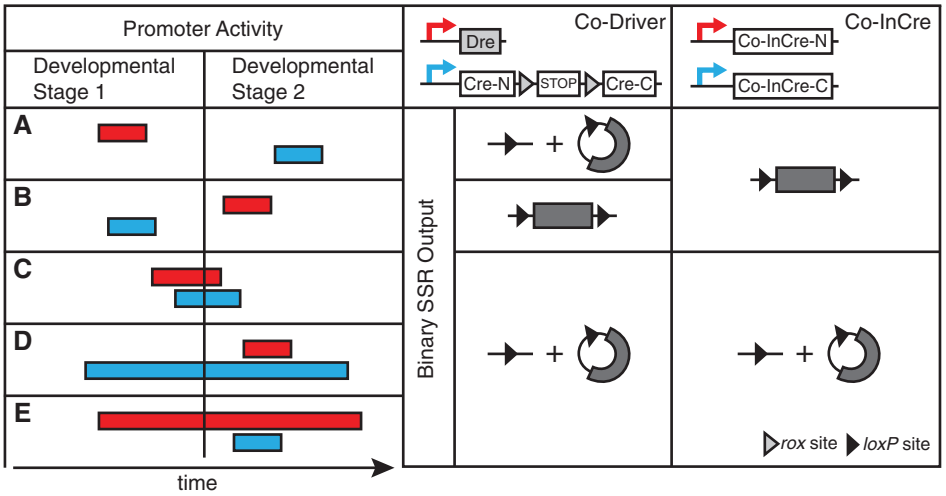

Figure 6. Binary Co-Driver and Co-InCre recombinase systems for sequential and coincidental conditional transgenesis. The binary recombinase components are expressed using two promoters with distinct expression profiles (red and cyan arrows, top right). Hypothetical temporal sequences of promoter activities within two distinct developmental stages of a cell lineage are shown on the left. Once activated, Cre recombinase processes a generic *loxP*-flanked responder sequence (dark gray box, processing is indicated by a linear and a circular reaction product), which could either represent a floxed exon leading to gene ablation or a floxed STOP cassette resulting in expression of a transgene. Non-overlapping expression patterns **(A, B)** result in recombination of *loxP* sites by Co-Driver only when Dre is expressed first (A). Both Co-Driver and Co-InCre yield recombination of *loxP* sites in the case of coincidental promoter activation with similar **(C)** or different **(D, E)** durations of transcription from the individual promoters.

with each other's recognition sites. Linking SSRs in series could, for example, be used to connect several SSR-based genetic logic circuits (46,47) to obtain higher order logic devices for synthetic biology applications in bacteria and mammalian cells. Second, we have constructed Co-InCre, a coincidental binary SSR system employing highly active split-inteins to reconstitute a native Cre polypeptide from N- and C-terminal precursors upon their simultaneous expression. Co-InCre showed unprecedented activity particularly in low-expressing transfected cells with a 2.5-fold increase in recombination efficiency of a genomic target relative to other binary SSRs tested. The improvement in recombination efficiency of Co-InCre over the recently published DnaE-based split-intein-split-Cre (9) most likely results from the combined effects of higher expression levels facilitated by codon-optimized Cre (22) sequences together with seamless and faster protein-splicing activity of the gp41-1 split-intein (15). In combination with simultaneously active promoters, Co-InCre most likely provides faster kinetics by reconstituting Cre on a protein level than sequential binary SSRs, which rely on two individual recombinases and thus on two subsequent cycles of transcription and translation.

Since its discovery, Cre recombinase has been unrivaled in creating tissue-specific driver lines and most complications observed in Cre-mediated conditional transgenesis seem to be related to the choice of promoters and design of expression cassettes rather than intrinsic Cre SSR activity (48). Our aim was to generate binary SSRs with the highest possible activity and therefore we focused on optimizing recombination efficiency in standardized model systems that allowed direct comparison with Cre. This strategy should result in dual-promoter-driven conditional transgenic animals that match the advantageous characteristics of many Cre driver lines. However, just as in the case of Cre, not every promoter combination will result in informative recombination patterns. Conversely, for certain populations of cells a strategy incorporating binary SSRs expressed from two intersectional strong promoters might be superior to Cre being controlled by a single promoter that is specific but low in transcriptional output.

The need for identifying cell sub-populations with an increased resolution is highlighted by the continuous improvements of histological methods (49) and flow cytometry (50) with the goal to increase the number of markers that can be analyzed simultaneously. We expect that high-resolution lineage tracing will complement these efforts with its unique capacity to create genetic records of developmental transitions. This will facilitate the inference of relationships between precursor and differentiated cells or cells that undergo transdifferentiation processes, which is difficult to conclude from immunodetection methods capturing only the current state of expressed markers. For certain biological questions temporal control of binary SSR function might be required. Ligand-dependent variants of all Co-Driver and Co-InCre components can be created with suitable solutions reported in the form of CreERT2 (3), DrePBD* (14), Split-CreERT2 (5) and more recently trimethoprim-controlled destabilized Cre (51).

Performing binary SSR-based lineage tracing requires the generation of mice that, including the Cre-responsive gene, harbor at least three transgenes. Recent advances in genome editing technologies such as combinations of ZFN (52–54) or TALEN (55) with plasmid-based targeting constructs promise the rapid generation of animals with targeted integration of Co-Driver or Co-InCre components into genomic loci providing suitable expression profiles. Potentially, a binary SSR founder animal

can be produced in one step by CRISPR/Cas9-mediated multiplexed genome editing in the mouse embryo (56).

SUPPLEMENTARY DATA

Supplementary Data are available at NAR Online.

ACKNOWLEDGEMENTS

We thank C. Monetti for kindly providing us with the Dre recombinase construct. We thank J. Hirrlinger for kindly providing us with the Split-Cre plasmids and K. Araki for kindly providing us with the CAG-CAT-STOP-cassette plasmid. The authors are grateful to G. Pilz, A. Senatore, A. Aguzzi, T. Buch, C. Wolfrum, S. Jessberger, R. Kelsh and L. Sommer for insightful discussions, and to M. Tarnowska, C. Albrecht and E. Skoczylas for excellent technical support.

FUNDING

The Swiss National Science Foundation [CRSI33 125073 to P.P.]; European Molecular Biology Organization [AST140-2013 and Fundacion La Caixa to D.S.]; Spanish Ministry of Economy and Competitiveness [BIO2012-39980 to L.M.]; European Research Council [DHISP250128 to H.U.Z.]. Funding for open access charge: University of Zurich.

Conflict of interest statement. None declared.

REFERENCES

1. Nagy,A. (2000) Cre recombinase: the universal reagent for genome tailoring. *Genesis*, **26**, 99–109.
2. Gong,S., Zheng,C., Doughty,M.L., Losos,K., Didkovsky,N., Schambra,U.B., Nowak,N.J., Joyner,A., Leblanc,G., Hatten,M.E. *et al*. (2003) A gene expression atlas of the central nervous system based on bacterial artificial chromosomes. *Nature*, **425**, 917–925.
3. Feil,R., Wagner,J., Metzger,D. and Chambon,P. (1997) Regulation of Cre recombinase activity by mutated estrogen receptor ligand-binding domains. *Biochem. Biophys. Res. Commun.*, **237**, 752–757.
4. Casanova,E., Lemberger,T., Fehsenfeld,S., Mantamadiotis,T. and Schutz,G. (2003) Alpha complementation in the Cre recombinase enzyme. *Genesis*, **37**, 25–29.
5. Hirrlinger,J., Requardt,R.P., Winkler,U., Wilhelm,F., Schulze,C. and Hirrlinger,P.G. (2009) Split-CreERT2: temporal control of DNA recombination mediated by split-Cre protein fragment complementation. *PLoS One*, **4**, e8354.
6. Hirrlinger,J., Scheller,A., Hirrlinger,P.G., Kellert,B., Tang,W., Wehr,M.C., Goebbels,S., Reichenbach,A., Sprengel,R., Rossner,M.J. *et al*. (2009) Split-cre complementation indicates coincident activity of different genes in vivo. *PLoS One*, **4**, e4286.
7. Jullien,N., Goddard,I., Selmi-Ruby,S., Fina,J.L., Cremer,H. and Herman,J.P. (2007) Conditional transgenesis using Dimerizable Cre (DiCre). *PLoS One*, **2**, e1355.
8. Jullien,N., Sampieri,F., Enjalbert,A. and Herman,J.P. (2003) Regulation of Cre recombinase by ligand-induced complementation of inactive fragments. *Nucleic Acids Res.*, **31**, e131.
9. Wang,P., Chen,T., Sakurai,K., Han,B.X., He,Z., Feng,G. and Wang,F. (2012) Intersectional Cre driver lines generated using split-intein mediated split-Cre reconstitution. *Sci. Rep.*, **2**, 497.
10. Dymecki,S.M., Ray,R.S. and Kim,J.C. (2010) Mapping cell fate and function using recombinase-based intersectional strategies. *Methods Enzymol.*, **477**, 183–213.
11. Madisen,L., Zwingman,T.A., Sunkin,S.M., Oh,S.W., Zariwala,H.A., Gu,H., Ng,L.L., Palmiter,R.D., Hawrylycz,M.J., Jones,A.R. *et al*. (2010) A robust and high-throughput Cre reporting and characterization system for the whole mouse brain. *Nat. Neurosci.*, **13**, 133–140.
12. Skarnes,W.C., Rosen,B., West,A.P., Koutsourakis,M., Bushell,W., Iyer,V., Mujica,A.O., Thomas,M., Harrow,J., Cox,T. *et al*. (2011) A conditional knockout resource for the genome-wide study of mouse gene function. *Nature*, **474**, 337–342.
13. Sauer,B. and McDermott,J. (2004) DNA recombination with a heterospecific Cre homolog identified from comparison of the pac-c1 regions of P1-related phages. *Nucleic Acids Res.*, **32**, 6086–6095.
14. Anastassiadis,K., Fu,J., Patsch,C., Hu,S., Weidlich,S., Duerschke,K., Buchholz,F., Edenhofer,F. and Stewart,A.F. (2009) Dre recombinase, like Cre, is a highly efficient site-specific recombinase in *E. coli*, mammalian cells and mice. *Dis. Model. Mech.*, **2**, 508–515.
15. Carvajal-Vallejos,P., Pallisse,R., Mootz,H.D. and Schmidt,S.R. (2012) Unprecedented rates and efficiencies revealed for new natural split inteins from metagenomic sources. *J. Biol. Chem.*, **287**, 28686–28696.
16. Dassa,B., London,N., Stoddard,B.L., Schueler-Furman,O. and Pietrokovski,S. (2009) Fractured genes: a novel genomic arrangement involving new split inteins and a new homing endonuclease family. *Nucleic Acids Res.*, **37**, 2560–2573.
17. Zhuo,L., Sun,B., Zhang,C.L., Fine,A., Chiu,S.Y. and Messing,A. (1997) Live astrocytes visualized by green fluorescent protein in transgenic mice. *Dev. Biol.*, **187**, 36–42.
18. Caroni,P. (1997) Overexpression of growth-associated proteins in the neurons of adult transgenic mice. *J. Neurosci. Methods*, **71**, 3–9.
19. Engler,C., Kandzia,R. and Marillonnet,S. (2008) A one pot, one step, precision cloning method with high throughput capability. *PLoS ONE*, **3**, e3647.
20. Cho,W., Hagemann,T.L., Johnson,D.A., Johnson,J.A. and Messing,A. (2009) Dual transgenic reporter mice as a tool for monitoring expression of glial fibrillary acidic protein. *J. Neurochem.*, **110**, 343–351.
21. Feng,G., Mellor,R.H., Bernstein,M., Keller-Peck,C., Nguyen,Q.T., Wallace,M., Nerbonne,J.M., Lichtman,J.W. and Sanes,J.R. (2000) Imaging neuronal subsets in transgenic mice expressing multiple spectral variants of GFP. *Neuron*, **28**, 41–51.
22. Shimshek,D.R., Kim,J., Hubner,M.R., Spergel,D.J., Buchholz,F., Casanova,E., Stewart,A.F., Seeburg,P.H. and Sprengel,R. (2002) Codon-improved Cre recombinase (iCre) expression in the mouse. *Genesis*, **32**, 19–26.
23. Xu,J. (2005) Preparation, culture, and immortalization of mouse embryonic fibroblasts. *Curr. Protoc. Mol. Biol.*, **Chapter 28**, Unit 28.21.
24. Mediavilla,J., Jain,S., Kriakov,J., Ford,M.E., Duda,R.L., Jacobs,W.R. Jr, Hendrix,R.W. and Hatfull,G.F. (2000) Genome organization and characterization of mycobacteriophage Bxb1. *Mol. Microbiol.*, **38**, 955–970.
25. Ghosh,P., Kim,A.I. and Hatfull,G.F. (2003) The orientation of mycobacteriophage Bxb1 integration is solely dependent on the central dinucleotide of attP and attB. *Mol. Cell*, **12**, 1101–1111.
26. Ghosh,P., Pannunzio,N.R. and Hatfull,G.F. (2005) Synapsis in phage Bxb1 integration: selection mechanism for the correct pair of recombination sites. *J. Mol. Biol.*, **349**, 331–348.
27. Nern,A., Pfeiffer,B.D., Svoboda,K. and Rubin,G.M. (2011) Multiple new site-specific recombinases for use in manipulating animal genomes. *Proc. Natl Acad. Sci. USA*, **108**, 14198–14203.
28. Grindley,N.D., Whiteson,K.L. and Rice,P.A. (2006) Mechanisms of site-specific recombination. *Annu. Rev. Biochem.*, **75**, 567–605.
29. Araki,K., Araki,M., Miyazaki,J. and Vassalli,P. (1995) Site-specific recombination of a transgene in fertilized eggs by transient expression of Cre recombinase. *Proc. Natl Acad. Sci. USA*, **92**, 160–164.

30. Andreas,S., Schwenk,F., Kuter-Luks,B., Faust,N. and Kuhn,R. (2002) Enhanced efficiency through nuclear localization signal fusion on phage PhiC31-integrase: activity comparison with Cre and FLPe recombinase in mammalian cells. *Nucleic Acids Res.*, **30**, 2299–2306.
31. Soriano,P. (1999) Generalized lacZ expression with the ROSA26 Cre reporter strain. *Nat. Genet.*, **21**, 70–71.
32. Greig,L.C., Woodworth,M.B., Galazo,M.J., Padmanabhan,H. and Macklis,J.D. (2013) Molecular logic of neocortical projection neuron specification, development and diversity. *Nat. Rev. Neurosci.*, **14**, 755–769.
33. Kriegstein,A. and Alvarez-Buylla,A. (2009) The glial nature of embryonic and adult neural stem cells. *Annu. Rev. Neurosci.*, **32**, 149–184.
34. Saito,T. and Nakatsuji,N. (2001) Efficient gene transfer into the embryonic mouse brain using in vivo electroporation. *Dev. Biol.*, **240**, 237–246.
35. Tabata,H. and Nakajima,K. (2001) Efficient in utero gene transfer system to the developing mouse brain using electroporation: visualization of neuronal migration in the developing cortex. *Neuroscience*, **103**, 865–872.
36. Langevin,L.M., Mattar,P., Scardigli,R., Roussigne,M., Logan,C., Blader,P. and Schuurmans,C. (2007) Validating in utero electroporation for the rapid analysis of gene regulatory elements in the murine telencephalon. *Dev. Dyn.*, **236**, 1273–1286.
37. Szymczak,A.L., Workman,C.J., Wang,Y., Vignali,K.M., Dilioglou,S., Vanin,E.F. and Vignali,D.A. (2004) Correction of multi-gene deficiency in vivo using a single 'self-cleaving' 2A peptide-based retroviral vector. *Nat. Biotechnol.*, **22**, 589–594.
38. Subach,O.M., Gundorov,I.S., Yoshimura,M., Subach,F.V., Zhang,J., Gruenwald,D., Souslova,E.A., Chudakov,D.M. and Verkhusha,V.V. (2008) Conversion of red fluorescent protein into a bright blue probe. *Chem. Biol.*, **15**, 1116–1124.
39. Malatesta,P., Hack,M.A., Hartfuss,E., Kettenmann,H., Klinkert,W., Kirchhoff,F. and Gotz,M. (2003) Neuronal or glial progeny: regional differences in radial glia fate. *Neuron*, **37**, 751–764.
40. Livet,J., Weissman,T.A., Kang,H., Draft,R.W., Lu,J., Bennis,R.A., Sanes,J.R. and Lichtman,J.W. (2007) Transgenic strategies for combinatorial expression of fluorescent proteins in the nervous system. *Nature*, **450**, 56–62.
41. Kelley,K.A., Friedrich,V.L. Jr, Sonshine,A., Hu,Y., Lax,J., Li,J., Drinkwater,D., Dressler,H. and Herrup,K. (1994) Expression of Thy-1/lacZ fusion genes in the CNS of transgenic mice. *Brain Res. Mol. Brain Res.*, **24**, 261–274.
42. Campsall,K.D., Mazerolle,C.J., De Repentingy,Y., Kothary,R. and Wallace,V.A. (2002) Characterization of transgene expression and Cre recombinase activity in a panel of Thy-1 promoter-Cre transgenic mice. *Dev. Dyn.*, **224**, 135–143.
43. Schepers,A.G., Snippert,H.J., Stange,D.E., van den Born,M., van Es,J.H., van de Wetering,M. and Clevers,H. (2012) Lineage tracing reveals Lgr5+ stem cell activity in mouse intestinal adenomas. *Science*, **337**, 730–735.
44. Buch,T., Heppner,F.L., Tertilt,C., Heinen,T.J., Kremer,M., Wunderlich,F.T., Jung,S. and Waisman,A. (2005) A Cre-inducible diphtheria toxin receptor mediates cell lineage ablation after toxin administration. *Nat. Methods*, **2**, 419–426.
45. Wu,S., Wu,Y. and Capecchi,M.R. (2006) Motoneurons and oligodendrocytes are sequentially generated from neural stem cells but do not appear to share common lineage-restricted progenitors in vivo. *Development*, **133**, 581–590.
46. Bonnet,J., Yin,P., Ortiz,M.E., Subsoontorn,P. and Endy,D. (2013) Amplifying genetic logic gates. *Science*, **340**, 599–603.
47. Siuti,P., Yazbek,J. and Lu,T.K. (2013) Synthetic circuits integrating logic and memory in living cells. *Nat. Biotechnol.*, **31**, 448–452.
48. Schmidt-Supprian,M. and Rajewsky,K. (2007) Vagaries of conditional gene targeting. *Nat. Immunol.*, **8**, 665–668.
49. Gerner,M.Y., Kastenmuller,W., Ifrim,I., Kabat,J. and Germain,R.N. (2012) Histo-cytometry: a method for highly multiplex quantitative tissue imaging analysis applied to dendritic cell subset microanatomy in lymph nodes. *Immunity*, **37**, 364–376.
50. Bendall,S.C., Simonds,E.F., Qiu,P., Amir,E.A.D., Krutzik,P.O., Finck,R., Bruggner,R.V., Melamed,R., Trejo,A., Ornatsky,O.I. *et al.* (2011) Single-cell mass cytometry of differential immune and drug responses across a human hematopoietic continuum. *Science*, **332**, 687–696.
51. Sando,R. 3rd, Baumgaertel,K., Pieraut,S., Torabi-Rander,N., Wandless,T.J., Mayford,M. and Maximov,A. (2013) Inducible control of gene expression with destabilized Cre. *Nat. Methods*, **10**, 1085–1088.
52. Cui,X., Ji,D., Fisher,D.A., Wu,Y., Briner,D.M. and Weinstein,E.J. (2011) Targeted integration in rat and mouse embryos with zinc-finger nucleases. *Nat. Biotechnol.*, **29**, 64–67.
53. Hermann,M., Maeder,M.L., Rector,K., Ruiz,J., Becher,B., Burki,K., Khayter,C., Aguzzi,A., Joung,J.K., Buch,T. *et al.* (2012) Evaluation of OPEN zinc finger nucleases for direct gene targeting of the ROSA26 locus in mouse embryos. *PLoS One*, **7**, e41796.
54. Meyer,M., de Angelis,M.H., Wurst,W. and Kuhn,R. (2010) Gene targeting by homologous recombination in mouse zygotes mediated by zinc-finger nucleases. *Proc. Natl Acad. Sci. USA*, **107**, 15022–15026.
55. Wang,H., Hu,Y.C., Markoulaki,S., Welstead,G.G., Cheng,A.W., Shivalila,C.S., Pyntikova,T., Dadon,D.B., Voytas,D.F., Bogdanove,A.J. *et al.* (2013) TALEN-mediated editing of the mouse Y chromosome. *Nat. Biotechnol.*, **31**, 530–532.
56. Yang,H., Wang,H., Shivalila,C.S., Cheng,A.W., Shi,L. and Jaenisch,R. (2013) One-step generation of mice carrying reporter and conditional alleles by CRISPR/Cas-mediated genome engineering. *Cell*, **154**, 1370–1379.